

A BIOMIMETIC AND BIOMECHANICAL APPROACH FOR TISSUE ENGINEERING

Hybrid Nanomaterials and a Piezoelectric Tunable Bending Apparatus for Mechanically Stimulated Osteoblast Cells Growth

Antonio Apicella and Raffaella Aversa

*Material Lab, Dept. of Cultura del Progetto, Specialistic School of Industrial Design for Innovation,
Second University of Naples, Aversa, Italy*

Keywords: Biomimetics, Biomechanics, Hybrid nanostructured biomaterials, Piezoelectric.

Abstract: The research develops and tests new hybrid biomimetic materials that work as mechanically stimulating "scaffolds" to promote early regeneration in implanted bone healing phases. A biomimetic nanostructured osteoconductive material coated apparatus is presented. Bioinspired approaches to materials and templated growth of hybrid networks using self-assembled hybrid organic-inorganic interfaces is finalized to extend the use of hybrids in the medical field. Combined *in vivo*, *in vitro* and computer-aided simulations have been carried out. Such multidisciplinary approach allowed us to explore many novel ideas in modelling, design and fabrication of new nanostructured biomaterials and scaffolds with enhanced functionality and improved interaction with OB cells. *In vivo* tests of Titanium screw implanted in rabbit tibiae have shown that mechanical stimulation was induced by the presence of bioactive hybrid perimplantar scaffold resulting in a differentiation and development of mesenchymal tissues. In order to investigate the relationship between bone growth and applied mechanical loading (strain), a piezoelectrically driven cantilever and a computer-controlled apparatus for "*in vitro*" tests has been developed and presented.

1 INTRODUCTION

Developing innovative tissue engineering biomimetic materials based on hydrophilic polymers has been extensively studied in the past decades on their physical, biological and mechanical properties. Although hard in the dry state, such polymers swell in water turning to soft and flexible materials used in several biomedical applications such as ophthalmic lenses, vascular prostheses, drug delivery system and soft-tissue replacement (Montheard et al., 1992; Apicella et al., 1993). Improved cytocompatibility in terms of cell adhesion and metabolism for IPN of HEMA and PCL was explained in terms of increased surface hydrophobicity leading to improvement of cell adhesion and spreading (Schiraldi et al., 2004). Highly biocompatible novel hybrid materials based on fumed silica and hydrophilic poly-(hydroxy-ethyl-methacrylate) (pHEMA) have been developed by the authors (Schiraldi et al., 2004). The addition of fumed silica is expected to improve the organization of the

polymeric network promoting hydrogen bonding of the polymeric chains with the hydrophilic nanoparticles. The resulting nanocomposites consisted in more rigid transparent materials with surprisingly improved mechanical strength and cytocompatibility (Schiraldi et al., 2004) that overcome one of the major drawbacks in hydrogels applications associated with their poor mechanical strength. Early studies confirmed that the nanofilled hybrid composites possess biomimetic and osteoconductive properties that can be useful in the design of mechanically bioactive innovative scaffolding systems for Osteoblast (OB) growth (Schiraldi et al., 2004). In healthy conditions, modelling and remodelling collaborate to obtain a correct shape and function of bones. This condition is completely altered when bone is implanted with a rigid prosthesis (Aversa et al., 2009; Sorrentino et al., 2007). Loads on bones cause bone strains that generate signals that some OB cells can detect and respond to. Threshold ranges of such signals are genetically determined and are involved in the

control of modelling and remodelling (Sorrentino et al., 2007; Frost, 1990; Wolff, 1892; Frost, 1964; Frost, 1994). Early studies by Wolff (1892) stated that mechanics could determine changes in the architecture of bones (Wolff, 1892). In 1964 Frost expressed mathematically the reactions of the bone tissue to given stimuli to quantitatively assess bone deformations (Frost, 1964). Remodelling processes repair the damage removing and replacing the damaged tissues with new bone. Moreover, overloading (or under-loading) alters such phenomenon (Frost, 1994). Mechanically compatible hydrogels as scaffolding materials could increase prosthesis adaptation mechanisms introducing active interfaces that improve implant biomimetics while reproducing cartilage and ligaments bio-mechanical functions. Adaptive properties of bone benefit of use of biomimetic (biomechanically compatible and bioactive) scaffold bio-materials.

2 MATERIALS AND METHODS

Our Biomimetic and Biomechanical approach resulted from a parallel mechanical and physical characterization of new hybrid material coupled to the bio-mechanical Finite Element analysis of the biological system investigated (implanted bones). The mechanics of the “in vitro dynamic bender testing apparatus” were designed by using FEA analysis utilising the material properties of the swollen hybrid pHEMA based nanocomposites.

2.1 Materials

Commercial 2-hydroxyethyl methacrylate, was purchased from Sigma-Aldrich Chemicals Co., (St. Louis, MO, USA). Fumed silicon dioxide (Aerosil 300 Degussa, Germany) with a mean diameter of 7 nm and specific surface area of $300 \text{ m}^2 \cdot \text{g}^{-1}$ was utilized as the bioactive filler. The initiator, $\alpha\text{-}\alpha'$ azoisobutyronitrile (AIBN), was purchased from Fluka (Milan, Italy).

HEMA monomers were mixed with increasing amount of fumed silica (4 to 30% by volume), according to the procedures described in a previous work. The resin was poured in 10 mm diameter cylindrical moulds, polymerized in a forced air circulation oven set at 60°C for 24 hrs and finally postcured at 90°C for 1 h.

2.2 Sorption and Swelling Test

The cylindrical samples were used for the water and

isotonic saline (0.15 M NaCl) water solution sorption and swelling experiments. The solution uptakes were determined at equilibrium by gravimetric measurements in a 0.1 mg Mettler Toledo balance (Milan, Italy). The advancing swelling fronts in the anomalous Case II (Apicella and Hopfenberg, 1982) of the samples were monitored measuring the thickness of the un-swollen residual glassy core as a function of time.

The equilibrium sorption and swelling experiments were performed at 37°C (thermostatic water bath) until constant weight up-take was monitored (100 h).

2.3 Finite Elements Analysis

Finite Element Analysis (FEA) on models of the Titanium implanted bones (human mandible segment) and of the in vitro bender set-up was performed according to the following procedures.

2.3.1 Models Set-up

Implanted bone (human mandible section)

The solid models were generated using Solidwork 2007 software. Titanium implant and the surrounding part of a mandibular cortical and cancellous bone were modelled. The average anatomical dimensions of the maxillary bone were generated according to literature data (Schwartz-Dabney, 2003) as a cancellous core surrounded by 2.0 mm-thick cortical bone. The FE model was obtained by importing the solid models into ANSYS rel. 9.0 FEM software (Ansys Inc. Houston) using IGES format. The volumes were meshed with eight nodes brick with 3 degree of freedom per node, resulting in a 3D FE model made up of 31,240 elements and 35,841 nodes. The model was constrained at the top surface of the maxillary bone. Accuracy of the model was checked by convergence tests (Sorrentino et al., 2007).

Piezoelectric Bender

The geometry of the piezoelectric bender has been measured on the commercial product (see section 2.5) and transferred to the FE environment according to the procedures described for the implanted bone. A 3 mm thickness symmetrical layers of rubber hydrogel were modelled at the two piezoelectric bender surfaces (simulating a thick coating of our swollen pHEMA based hybrid composite)

2.3.2 Mechanical Properties of Materials

Orthotropic assumption for cortical bone was adopted while the cancellous bone was considered as isotropic linear materials. The Young's modulus and

Poisson's ratio of isotropic materials used in the models of the Titanium implanted bone and piezoelectric bender are shown in Table 1 (Schwartz-Dabney, 2003).

Table 1: Isotropic mechanical properties of materials.

	Young's modulus	Poisson's ratio
Cancellous bone	0.91 (GPa)	0.30
Titanium	110 (GPa)	0.30
Piezoelectric ceramic	400 (GPa)	0.15
Swollen pHEMA Hybrid nanocomposite	5 (MPa)	0.48

Cortical bone was divided into two sites, one on the buccal side and one on the palatal side according to the mechanical characterization reported for a dentate mandible by Schwartz- Dabney and Dechow (Schwartz-Dabney, 2003). Each area has its own orthotropic constants values and orientation of the maximum stiffness direction, the directions of the maximum stiffness is referred to the occlusal plane. E and G are expressed in GPa. Direction of maximum stiffness are referred to the global coordinate system. Orthotropic elastic constants and orientation for buccal and palatal sides of cortical bone are reported in Table 2.

Table 2: Orthotropic constants adopted for the cortical bone on the buccal and palatal sides, respectively.

	Max stiff.°	E1	E2	E3	G12	G31	G23	_12	_31	_23
facial	39.9	11	15	18	4.5	4.7	5.7	0.21	0.25	0.42
buccal	4.4	12	18	19	4.9	4.9	5.1	0.16	0.31	0.43

Local orientation of the maximum stiffness (E3) and the other two orthogonal stiffness directions (E1, E2) have been reproduced dividing the shell of external elements (compact bone structure) in orientation sites according to the proposed experimental mechanical characterization. The orientation of the maximum stiffness has been reproduced for each site by defining a local coordinate system and by orienting the site's elements coordinate systems accordingly.

The maximum stiffness (E3) directions in degree referred to the occlusal plane on buccal and palatal side are reported in Table 2. E1 direction is normal to the cortical surface.

2.4 Mechanical Characterization

Shear elastic modulus measurement on dry and swollen p-HEMA Hybrid nanocomposites were performed using a METTLERLEDO (Zurich, Switzerland) dynamical mechanical tester operating in shear mode (DMA). The elastic and viscous components of the shear modulus were measured

under constant frequency loading in isothermal condition. The samples were dried under vacuum at a 60°C for 24 h before testing. In the shear test mode, the 10 mm diameter and 2 mm thickness sample disks are placed between three steel plates forming a symmetrical sandwich. An isothermal scan at 37°C in a dry Nitrogen purged environment was performed. The deformation control was set to 10 µm and a force limitation of 0,9 N was applied at an oscillating frequency of 10 Hz.

2.5 Mechanical Controlled Bender

57 mm piezoelectric benders (Quick-Mount 503, PIEZO SYSTEMS, INC. Woburn, MA USA) were used to build the oscillating dynamic scaffold supports. A proprietary software and electronic apparatus was used to drive oscillating output voltage exit (0-100V). The deformations at the bender surface were monitored by acquisition data software (System 4000 with 20 input channels by Vishay Measurements Group Inc., NC, USA) at 2 points/s. The bender operates with max displacement of 1.0 mm.

2.6 In Vivo Osteointegration Tests

2 implants for each rabbit tibia, in 6 rabbits (total of 24 implants in New Zealand White rabbits); each rabbit has been implanted with 2 implants coated with the nanostructured hybrid biomaterial on the right tibia and 2 control implants in the left tibia. Micro Computer Tomography with resolution 1 voxel=15 cubic micron has been performed on the explanted tibiae after 1 week, 1, 2, 4 and 6 months. BV/TV (Bone Volume/Total Volume), BS/TV (Bone Surface), TbTh (Trabecular Thickness), TbSp (Trabecular Separation), TbN (Trabecular Number) have been used to evaluate the Total BIA (bone implant apposition).

3 DISCUSSION

The aim of our research was to develop a biomimetic/biomechanical approach for the design of the experimental dynamic procedures (biological-mechanical stimulus) finalized to favour adaptive directionally organized OB growth in vitro scaffold mineralization. In order to achieve this result, both a proper biomimetic scaffolding material and an externally driven mechanically straining apparatus have had to be designed.

The biomimetic characteristic of our hybrid materials have been investigated both for

mechanical than osteoconductive properties.

3.1 Bio-mimetics: Hybrid Nanocomposites Properties Design

Physiological bone material behaviour to be mimicked by the bio-active scaffolding material relates to the following aspects:

- mechanical properties (dry – swollen)
- bioactivity (in vivo tests)

In order to define the proper nanofiller/polymer ratio of potentially idoneous the hybrid nanocomposites The objective properties requirements are

- similar to bone rigidity (Elastic Modulus 6-15 GPa and shear modulus G 2-5 GPa) when dry
- similar to cartilage and ligament flexibility (Halpin and Kardos, 1976) (high deformability - Elastic modulus 2-20 MPa) when swollen.

3.1.1 Mechanical Properties

The dry Hybrid pHEMA nanocomposites with compositions ranging from 4 to 30% by volume of nanosilica were isothermally shear tested in a Dynamic Mechanical Analyser operating at 10Hz and at 37°C. The samples showed a predominantly elastic behaviour (the viscous component was negligible for all compositions). The values of the measured Shear moduli are reported in figure 1.

The compositional dependency of the shear modulus of the nanocomposites does not follow the ordinary Halpin-Tsai relationship utilized to describe the elastic properties of particulate composites (red line) (Töyräsa et al., 2001), while resembles to that of a 3D oriented fibre mat (green line in figure 1), indicating the formation of a continuous hybrid ceramo-polymeric structure. Shear moduli comparable to those of the cortical bone have been measured for nano-silica volumetric fractions ranging from 4 to 12%. A volume fraction of 5% has been then chosen for the in vivo osteointegration tests and for the FEA simulations.

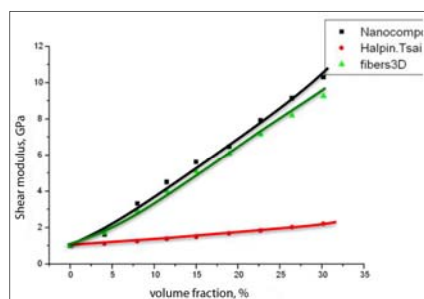


Figure 1: Hybrid shear moduli (black), Halpin-Tsai (red) and 3D fibres composite (silica glass fibres mat) (green).

3.1.2 Swelling and Sorption Behavior

The 5% hybrid nanocomposites dramatically swell in water solutions (figure 2) picking up 50% of its dry weight and reducing its shear modulus to 2-3 MPa (measured in the DMA). Such phenomenon is associated to the water induced polymer plasticization that reduces the polymer glass transition temperature below the test temperature



Figure 2: Swelling behaviour of the nanostructured hybrid scaffold material.

This behaviour has been investigated in a physiological isotonic 0.15 M NaCl solution held at 37°C for the 5% volume fraction sample both for equilibrium and swelling kinetic. Once exposed to the water solution, the initially dry and glassy pHEMA composite starts to swell showing a clear front dividing the rubber swollen external portion and the unaffected glassy core. This glassy core thickness progressively reduces as the swollen front advance through the sample (upper part of figure 3). A measure of the swelling kinetic is given by the rate of reduction of the glassy core as a function of the time (lower diagram in figure 3). The swelling front advances at constant rate: this behaviour is characteristic of a limiting relaxation controlled sorption mechanism indicated as “Case II sorption” (Apicella et al., 1993; Schiraldi et al. 2004; Aversa et al., Sorrentino et al., 2007; Frost, 1990; Wolff, 1892; Frost, 1964; Frost, 1994; Apicella and Hopfenberg, 1982). At equilibrium, when swelling fronts meet, a 14.5% increase of the sample diameter has been measured (about 50% of volume increase). The resulting swelling rate is of 0.10 mm per hr.

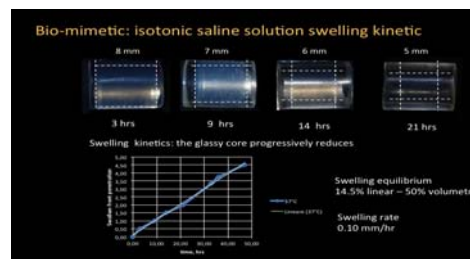


Figure 3: Swelling kinetic of a 5% by volume hybrid nanocomposite in 0.15M NaCl water solution (isotonic).

3.2 Bio-mechanics: Adaptive Properties of Bone

The use of biocompatible and biomechanically active interface that can be “designed” to reproduce bone compatible and biomimetic strain distribution is discussed in the present paper. The ranges of the physiological strains and related bone adaptive properties according to (Frost, 1990; Frost, 1994) are reported in figure 4. There are upper ($>3000\mu\epsilon$) and lower ($< 50\mu\epsilon$) strain limits that do not favour healthy bone growth.

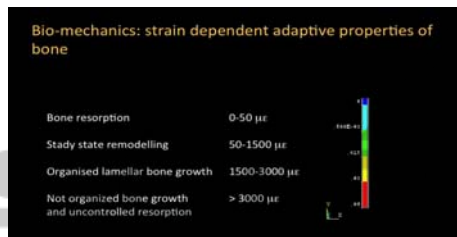


Figure 4: Adaptive properties of bone: strain ranges for bone resorption ($< 50\mu\epsilon$ blue), remodelling ($50-1500 \mu\epsilon$ light blue-green) and organized growth ($1500-3000\mu\epsilon$ yellow-red), resorption ($> 3000\mu\epsilon$).

The comparison between FEA simulation of physiological strains in coated and uncoated implants and bone volumes in the in rabbit tibiae after two months of in vivo test is reported in figure 5. The FEA simulations of the strain distribution reported of the same figure 5 have been run on a mandibular bone section that presents comparable to the rabbit tibia mechanical and dimensional characteristics.

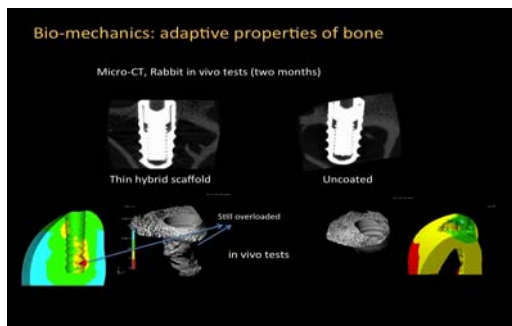


Figure 5: Osteointegration of Titanium implants with a nanostructured hybrid biomimetic coating (left side) and without (right). Micro-CT bone reconstruction and FEA calculated physiological strain distributions are compared.

The Micro CT bone reconstructions of the perimplantar areas of the hybrid nanostructured biomaterial coated and of the “as received” implants

after two months are compared in figure 5: the nanostructured biomaterial coated implant shows a better osteointegration that can be related to the osteoconductivity of the perimplantar biomimetic hybrid coating.

The bone implant apposition or bone ingrowth (COMERON, 1986), which is defined as the percentage of osteointegrated implant length for the biomimetically coated and uncoated implants in the six months in vivo test show a significant improvement of about 100% increase in the first two months and 30% after 6 months.

The Osteoblast proliferation and bone growth in the implanted tibiae is clearly favoured and accelerated by the presence of the hybrid nanostructured coating. The biomechanical approach using the adaptive properties of bone well describes the biomimetic behaviour of the proposed perimplantar hybrid scaffold since it can predict areas of bone resorption (FEA model elements with strains below the physiological lower limits have been removed in the image), as it occurs in the in vivo tests at the neck of the implant (Micro CT reconstruction on the right side of figure 5). The proposed biomechanical model can predict areas of bone growth (FEA model and micro CT reconstruction compared in the left side of figure 5). According to Frost:

1. Remodelling is triggered not by principal stress but by 'strains'.
2. Repetitive dynamic loads on bone trigger remodelling while static loads do not.

Dynamic factors have been accounted and utilized to design a piezoelectric driven dynamic scaffold deformation apparatus for in vitro adaptive osteoblast cells growth. Biomimetic aspects are investigated by using the osteoconductive hybrid nanocomposites bender thick swollen coating coupled with a FEM modelling of the in vitro bone adaptive growth. The piezoelectric dynamic bender and control system are shown in figure 6.

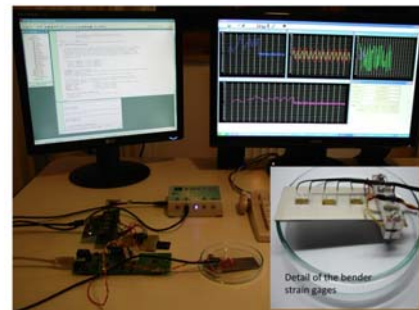


Figure 6: Piezoelectric bender for dynamic OB cells culture tests: calibration test configuration.

FEA results showing the distribution of the unidirectional strains in the x direction (EPSX) in the simulation of 1 mm oscillation at the free end in the controlled bending test is reported in figure 7. In the red-orange zone (1500 microepsilon), the strains are compatible with those inducing organized lamellar bone growth in healthy bone. OB colonization of the hybrid scaffold in the areas of biologically compatible straining is favoured.

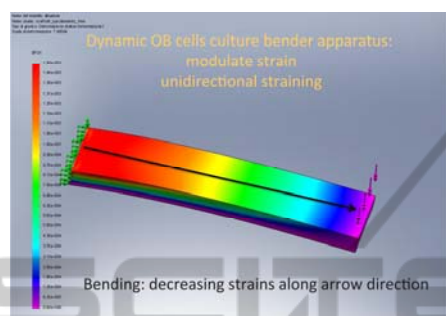


Figure 7: FEA for the evaluation of the unidirectional strains in the oscillation controlled bender.

The organized bone to grow in the red-orange area causes a localized increase of the ossified scaffold stiffness. Considering these localized time dependent stiffening in the material highly strained areas, a bone growing front moving in the direction of the arrow (figure 8) is generated.

The rigid growing bone front lets a new area of the scaffold to be bio-actively stimulated according to the physiological strain for steady state remodelling (50-1500 $\mu\epsilon$ - light blue and green areas) and organized lamellar bone growth (1500-3000 $\mu\epsilon$ - yellow-red areas). The oscillating straining apparatus, than, can be used in in vitro experiments to bone grow in thick scaffolds from OB cell culture (figure 8).

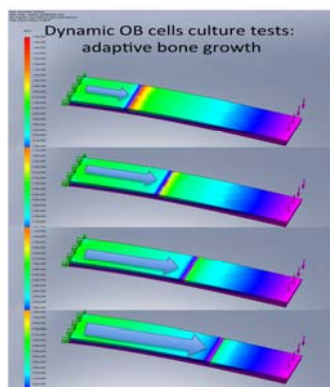


Figure 8: Dynamic FEA simulation of the advancing bone growth front under dynamic flexure straining conditions.

4 CONCLUSIONS

A biomimetic/biomechanical approach has been pursued in designing the experimental dynamic procedures (bio-mechanical stimuli) for in vitro scaffold mineralization and ossification using piezoelectric benders. The proposed material is a Nanocomposites - Hybrid ceramo-polymeric poly-Hydroxyl-Ethyl-Methacrylate (pHEMA) additioned with nanosilica particles (4-6% by volume). This biomimetic material swells in presence of physiological solution (when in a biological aqueous environment) picking-up to 50-30% by weight of water. Mechanical behaviour in the glassy state is comparable with bone while, in the swollen rubbery state, is comparable with those of cartilage and ligaments.

ACKNOWLEDGEMENTS

Funds from PRIN 2008 and FIRB (Funds for Base Research) Futuro in ricerca 2008.

REFERENCES

- Montheard JP, Chatzopoulos M, Chappard D. *J Macromol Sci Macromol Rev* 1992;32:1-34.
- Apicella A, et al. *Biomaterials* 1993;142:83-90.
- Schiraldi C, D, Apicella A, Aversa R, De Rosa M (2004) *Biomaterials* 25 (17):3645-3653.
- Aversa R, Apicella D, Apicella A (2009). *Dental materials* 2009; 25: 678-690
- Sorrentino R, Aversa R, Apicella A. *Dent Mater* 2007; 23: 983-93.
- Frost HM. *Anat Rec* 1990; 226:403-13.
- Wolff J. *Das Gesetz der Transformation der Knochen*. Berlin: A Hirschwald; 1892.
- Frost HM. *Mathematical elements of lamellar bone remodeling*. Springfield: C. C Thomas; 1964. pp. 22-25.
- Frost HM. *Angle Orthod* 1994; 64:175-88.
- Apicella A, Hopfenberg Hb. *Journal of Applied Polymer Science*, 1982; Vol. 27(4), P. 1139-1148, Issn: 0021-8995
- Schwartz-Dabney, C.L. (2003) *American Journal of Physical Anthropology* 120: 252-277.
- J Töyräsa, et al., *Journal of Biomechanics*, Volume 34, Issue 2, 2001, 251-256
- J.C. Halpin and J. L. Kardos; *Polymer Engineering and Science*, 1976, v16, N5, pp 344-352
- H. U. COMERON, *Clin. Orthop.* 208 (1986) 81